A R C H I V E S O F M E T A L L U R G Y A N D M A T E R I A L S
Volume 54 2009 Issue 1

T. BAUDIN*, Z. JASIEŃSKI**, R. PENELLE*, A. PIĄTKOWSKI**

CHARACTERISTICS OF TEXTURE EVOLUTION OF COPPER SINGLE CRYSTALS IN CHANNEL DIE COMPRESSION BY ELECTRON BACK SCATTERING DIFFRACTION

CHARAKTERYSTYKA LOKALNYCH ZMIAN TEKSTURY MONOKRYSZTAŁÓW MIEDZI ŚCISKANYCH W PŁASKIM STANIE ODKSZTAŁCENIA

Texture development of copper single crystals during plane strain compression is analyzed from individual measurements obtained by electron back scattered diffraction. The unstable (100)[011] and (111)[$\bar{1}\bar{2}$3] orientations are studied: the first one splits into complementary (112)[$\bar{1}\bar{1}$1] and ($\bar{1}\bar{1}$2)[111] stable orientations with a spreading towards the (114)[$\bar{2}\bar{2}$1] and the ($\bar{1}\bar{1}$4)[221] orientations, respectively. The (111)[$\bar{1}\bar{2}$3] crystal decomposes into the (112)[$\bar{1}\bar{1}$1] orientation with a spreading towards the (114)[$\bar{2}\bar{2}$1] orientation and the (110)[001] orientation that tends to rotate near the (110)[1$\bar{1}\bar{2}$] orientation, so as to become stable at higher strains. The use of individual orientation measurements allows one to determine the local orientations of two sets of symmetric coarse slip bands for the first single crystal, and to distinguish between the orientations of the crystal matrix and the coarse slip bands and the macroscopic shear bands which appear during the deformation for the second single crystal.

Rozwój tekstury monokryształów miedzi ściskanych w płaskim stanie odkształcenia jest analizowany w oparciu o metodę dyfrakcji odbitych elektronów wstecznych w mikroskopie skaningowym (metoda Electron Back Scattering Difraction). Badano orientacje (100)[011] – niestateczna oraz (111) [$\bar{1}\bar{2}$3]. Pierwsza z nich rozpada się na komplementarne i stabilne orientacje (112)[$\bar{1}\bar{1}$1] i ($\bar{1}\bar{1}$2)[111], które cechują się rozmyciem ku orientacjom odpowiednio : (114)[$\bar{2}\bar{2}$1] i ($\bar{1}\bar{1}$4)[221]. Natomiast monokryształ o orientacji (111) [$\bar{1}\bar{2}$3] rozpada się na fragmenty o orientacjach (112)[$\bar{1}\bar{1}$1] z rozmyciem do (114)[$\bar{2}\bar{2}$1] oraz o orientacji Gossa (110)[001], która ma tendencję do obrotu w położenie (110)[1$\bar{1}\bar{2}$] – tzw orientacja „mosiądzu", stała w zakresie dużych odkształceń. Zastosowanie metody pomiarów indywidualnych orientacji umożliwia określenie lokalnej orientacji dwóch symetrycznych zbiorów grubych pasm poślizgu (CSB) występujących w pierwszym monokrysztale o tzw „orientacji ścinania" oraz wyróżnienie orientacji osnowy, grubych pasm poślizgu i makroskopowych pasm ścinania, które występują podczas odkształcenia drugiego z kryształów o orientacji (111) [$\bar{1}\bar{2}$3].

1. Introduction

During tensile test of f.c.c single crystals, then plastic flow is localized in two modes [1,2,3] : (i) the coarse slip bands (CSBs) which develop at low strains, i.e. before necking (Considere's criterion), and (ii) the macroscopic (sample scale) shear bands (MSBs) appearing at large strains as a typical phenomena of the post-necking behaviour. Also, these CSBs and MSBs, both appear, at low or at large reductions, respectively, in rolling and/or in plane strain compression (channel-die). At the TEM scale both these inhomogeneities of deformation exhibit very similar internal dislocation microstructures which are composed of highly elongated cells and microbands clusters [1,4,5]. The relatively large local misorientation within the MSBs is the feature that distinguishes them from the CSBs [1,2,5,6]. For MSBs, the lattice inside the bands rotates typically by 10° to 20° away from the surrounding crystal lattice, and for CSBs the misorientations across the band are very small and these bands are closely aligned with the crystallographic slip planes of operative slip systems.

The lattice misorientation within the MSBs will affect the texture evolution. It will modify the relative importance of the β – fibre components of rolling texture of f.c.c. metals, since single crystals experiments [3,7,8] reveal a strong tendency to develop MSBs in the stable, the so-called C (or "copper"), (112)[$\bar{1}\bar{1}$1] orientation. Therefore, in a study by the authors [6] on (112)[$\bar{1}\bar{1}$1]

* UNIVERSITÉ DE PARIS SUD, LABORATOIRE DE MÉTALLURGIE STRUCTURALE, U.R.A. 1107, BÂTIMENT 413, 91405 ORSAY CEDEX, FRANCE
** INSTITUTE OF METALLURGY AND MATERIALS SCIENCE, POLISH ACADEMY OF SCIENCES, 30-059 KRAKÓW, 25 REYMONTA STR., POLAND

copper single crystals (see also Wagner et al. [9]), a particular effort has been made to cover the texture evolution over a wide range of scales by correlating the X-ray, neutron and electron back scattered diffraction (EBSD) [10] measurements on the same samples deformed in channel-die compression. It has been found that the C orientation can be considered as stable only in terms of average (global) texture, since the orientation splitting towards the (114)[$\bar{2}\bar{2}$1] and (116)[$\bar{3}\bar{3}$1] components of texture occurs as a consequence of the lattice rotation within the MSBs. The EBSD measurements [6] have shown that the lattice inside the MSBs is locally rotated away from the surrounding (112)[$\bar{1}\bar{1}$1] crystal matrix by 15° to 22° around the transverse direction.

This type of analysis has been applied to a more general case of copper crystals of unstable, high symmetry orientations, undergoing plane strain compression. In different parts of these crystals different sets of slip systems {111}< 110 > lead to locally diverging orientations. However, considering the texture similarity obtained by X-ray and neutron diffraction that indicates low influence of friction during the channel die test, and considering that these global textures and their evolution have already been discussed in literature, only the individual orientation measurements are presented. The work is hence specially focused on copper single crystals of the (001)[110] and (111)[$\bar{1}\bar{2}$3] orientations which decompose during rolling and channel-die compression into diverging orientations by lattice rotations of opposite sign [3, 4, 11-17]. The first of them is representative of the usual shear texture component of f.c.c. metals and the second one lies initially off the high symmetry (111)[$\bar{1}\bar{1}$2] orientation. In plane strain compression, these two orientations develop the strong C component of texture together with formation of the MSBs; they are therefore interesting from the point of view of local texture. The (001)[110] is assumed to be deformed by a symmetric slip on two pairs of coplanar systems (CP), each pair (CP1 and CP2) being localized in separate sets of the CSBs. Thus, it is important to distinguish the crystallographic orientation of each set of CSBs. The (111)[$\bar{1}\bar{2}$3] initial orientation deformation leads to the appearance of the two (112)[$\bar{1}\bar{1}$1] and (110)[1$\bar{1}\bar{2}$] orientations, and thus it appears interesting to define if the observed CSBs and MSBs contribute to the appearance of a particular or of the two described orientations.

2. Material and experimental techniques

Single crystals of high purity (99.994%) copper were prepared by the Bridgman method and sectioned into cubic samples (10 × 10 ×10 mm^3) with the initial (001)[110] and (111)[$\bar{1}\bar{2}$3] orientations. After electropolishing and coating with teflon films used as a lubricant, the samples were deformed, at a strain rate of 5.10^{-4} s^{-1}, in channel-die compression (fig. 1) to several (logarithmic) strains (table 1). Using the von Mises criterion, the equivalent strains were calculated; $\overline{\varepsilon} = 2/\sqrt{3}\ \ln H_0$, where H_0 is the initial height and H is the height at the time t.

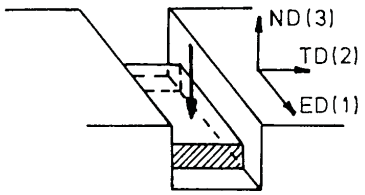

Fig. 1. Scheme of the channel die test

The individual orientations measurements by EBSD were carried out on the lateral face of the crystals (ND/ED plane: ND: normal direction, ED: direction of elongation, TD: transverse direction) and the corresponding {111} pole figures were plotted on the compression plane. In the EBSD, the spatial resolution is about 0.5 m, and the orientations were determined with a precision of about 1-2 degrees.

Obviously, the EBSD technique is particularly interesting if one tries to distinguish the crystallographic orientations within the slip or shear bands from those of the crystal matrix. However, in the present study, another approach has been also used. It consists in a masking of the matrix with Pb sheets of 0.5mm thickness to permit the X-ray measurements (fig. 2) of local texture within MSBs which appears during the deformation of the (111)[$\bar{1}\bar{2}$3] initial orientation. Let us note that this last technique is possible because the width of a set of MSBs in channel-die compressed crystals is great enough (about 4000 × 1000 μm^2).

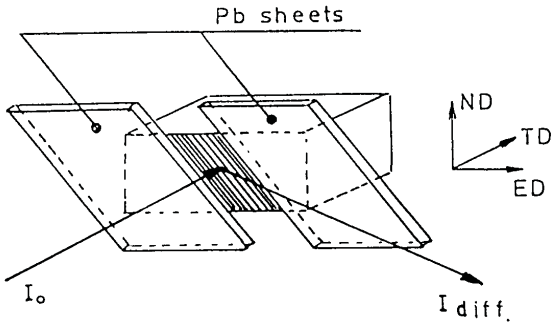

Fig. 2. Scheme of the technique of measuring the texture inside of a MSB by X-ray diffraction

Slip and shear band patterns were observed by optical microscopy on the longitudinal sections for all reductions.

3. Texture of copper single crystals deformed in plane strain compression

3.1. The (001)[110] orientation

The evolution of the (001)[110] orientation during the compression is shown schematically in figure 3. This evolution can be simply described by rotations around TD, first, of about ± 20° to obtain the (114)[$\bar{2}\bar{2}$1] and ($\bar{1}\bar{1}$4)[221] orientations, and then of about ± 15° which corresponds to the transformation from the (114)[$\bar{2}\bar{2}$1] and ($\bar{1}\bar{1}$4)[221] orientations, respectively, to the (112)[$\bar{1}\bar{1}$1] and ($\bar{1}\bar{1}$2)[111] ones : that is a total rotation of about ± 35°. Similar behaviour is shown by Akef and Driver [11] and Becker et al. [12] for aluminium single crystals.

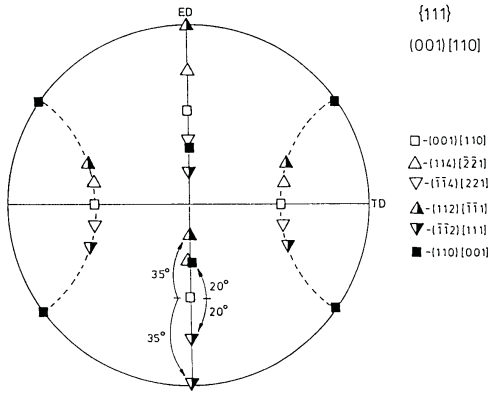

Fig. 3. Evolution of the (001)[110] initial orientation during deformation

During the deformation of the (001)[110] initial orientation, two pairs of ($\bar{1}\bar{1}$1)[101]+[011] and (111)[$\bar{1}$01]+[0$\bar{1}$1] symmetric coplanar CP slip systems are active. These two pairs of CP slip systems (CP1 and CP2 respectively) lead by a heterogeneous or "patchy" slip to symmetric orientations which evolve from (114)[$\bar{2}\bar{2}$1] to (112)[$\bar{1}\bar{1}$1], and from ($\bar{1}\bar{1}$4)[221] to ($\bar{1}\bar{1}$2)[111] as the deformation proceeds. The resulting deformation is perfectly aligned with the channel, because the net shearing directions associated with two symmetrical families of active CP slip systems are then [112] in ($\bar{1}\bar{1}$1), and [$\bar{1}\bar{1}$2] in (111). Figure 4 shows an example of a "patchy" slip at low strains ($\overline{\varepsilon}$=0.33). Two sets of slip traces make an angle of about 40° with the ED, which confirms the initial orientation change towards (116)[$\bar{3}\bar{3}$1] and ($\bar{1}\bar{1}$6)[331] with a tendency to comprise the (114)[$\bar{2}\bar{2}$1] and ($\bar{1}\bar{1}$4)[221] by global rotation about TD close to [$\bar{1}$10]. For these orientations, the slip planes (111) and ($\bar{1}\bar{1}$1) of the active CP systems made a 39° (for {116}<331>) or a 35° (for {114}<221>) angle with ED. Next, when the two (112)[$\bar{1}\bar{1}$1] and ($\bar{1}\bar{1}$2)[111] symmetric components of texture appear two separate sets of CSBs, which make about 20° with ED, are observed (fig. 5). As discussed by Harren et al. [1], and confirmed by Jasienski et al. [3,4], each pair of a CP slip system is located in a separate set of CSBs which consists of microbands clusters in the octahedral plane of an operative CP slip system.

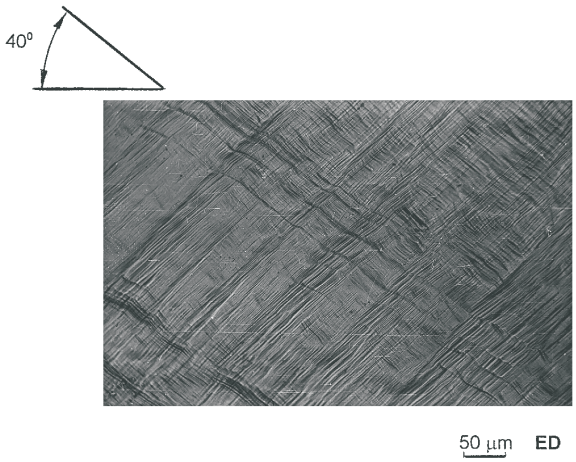

Fig. 4. (001)[110] initial orientation. Micrograph of the "patchy" slip at $\overline{\varepsilon}$ = 0.33

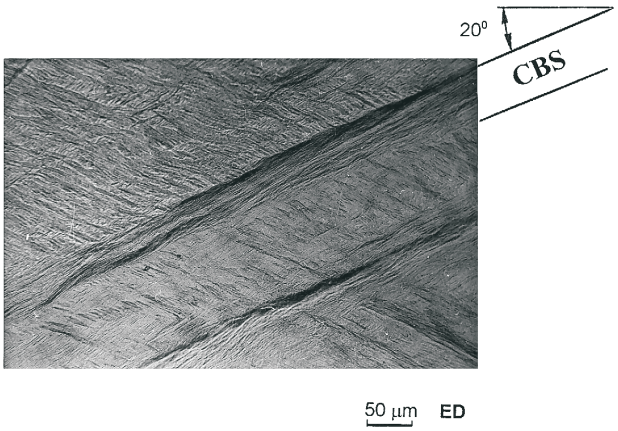

Fig. 5. (001)[110] initial orientation. Micrograph of a separate set of CSBs ($\overline{\varepsilon}$ = 0.95)

This correlation can be verified measuring separately the local orientation inside of each set of CSBs by EBSD. The {111} pole figures determined on samples deformed at $\overline{\varepsilon}$=0.45 and $\overline{\varepsilon}$=1.82 are shown in figures 6a and 6b, respectively. The results confirm that each set of CSBs has symmetric orientations which change from the (001)[110] initial orientation to the (114)[$\bar{2}\bar{2}$1] and

$(\bar{1}\bar{1}4)[221]$ orientations at $\overline{\varepsilon}$=0.45, and to the $(112)[\bar{1}\bar{1}1]$ and $(\bar{1}\bar{1}2)[111]$ orientations at $\overline{\varepsilon}$=1.82. So, the local texture within CSBs corresponds to the average texture of deformed matrix [3,4] determined by X-ray and neutron diffraction measurements.

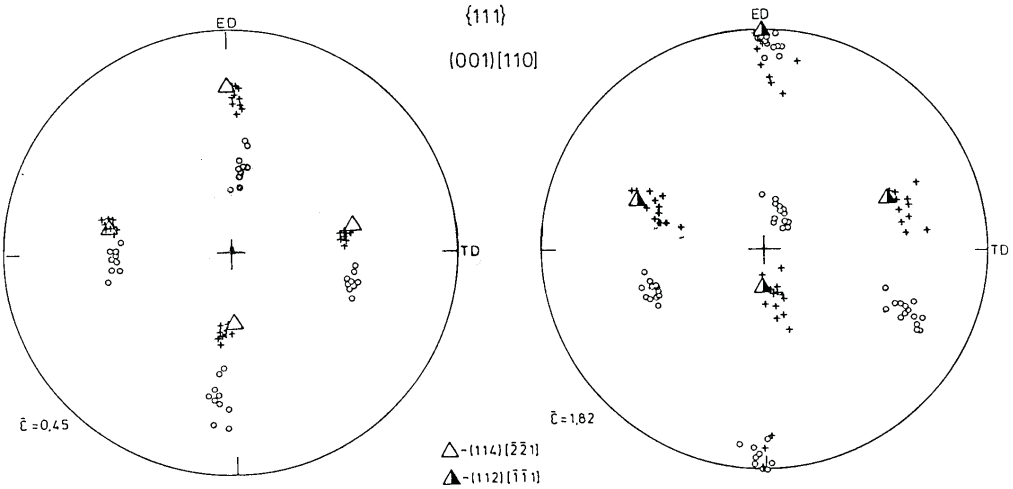

Fig. 6. (001)[110] initial orientation. {111} pole figures measured by EBSD for the strains : (a) $\overline{\varepsilon}$=0.45, (b) $\overline{\varepsilon}$=1.82

The MSBs which develop in C orientation at strain of about 1.5 (fig. 7) are deviated apparently by 15° to 20° from the CSBs plane, i.e. the nearest critically stressed octahedral slip plane. The increase of the strain increases the volume fraction of the MSBs, though the main component $(112)[\bar{1}1]$ (or $(\bar{1}\bar{1}2)[111]$ of average texture remains unchanged up to about 80 pct of reduction ($\overline{\varepsilon}$=1.82) [3]. Only a local spreading toward the $(114)[\bar{2}\bar{2}1]$ (or $(\bar{1}\bar{1}4)[221]$) orientation inside the MSBs is observed in figure 6b. Morii et al. [7] also observed that the $(211)[\bar{1}11]$ Al and Al-Mg crystals rolled up to 90 pct of reduction ($\overline{\varepsilon}$=2.66) were stable although orientation fluctuations corresponding to a rotation around the TD appeared. Similar orientation changes towards the (001)[110] inside the MSBs of a cold rolled $(112)[\bar{1}\bar{1}1]$ copper single crystals have been also reported by Wagner et al. [9]. Such misorientations indicate that inside the MSBs, the critically stressed coplanar slip planes (111) rotate back against the rigid body rotation of the deformed matrix, thus the resolved shear stress increases on the (111) and $(\bar{1}\bar{1}1)$ planes.

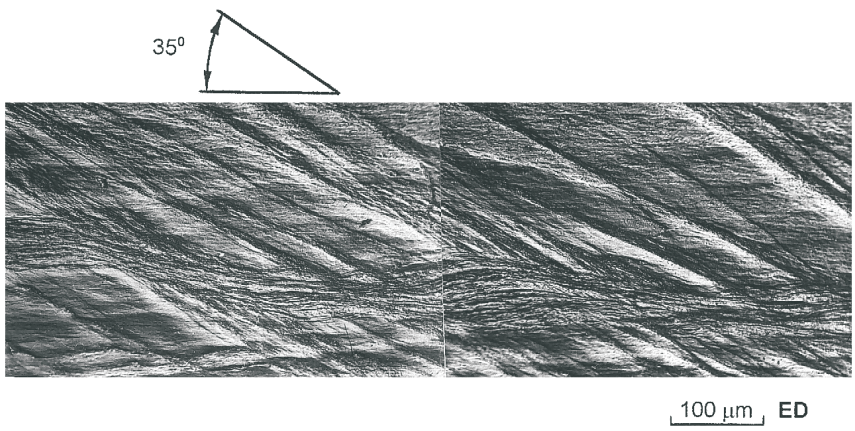

Fig. 7. Micrograph of a separate set of MSBs ($\overline{\varepsilon}$=2.0)

When the (112)[$\bar{1}\bar{1}1$] (and ($\bar{1}\bar{1}2$)[111]) orientation is reached, the ($\bar{1}11$)+(1$\bar{1}$1)[110] (and ($\bar{1}11$)+(1 $\bar{1}$1)[$\bar{1}\bar{1}$0]) co-directional (CD) systems and the already present (111)[$\bar{1}$1]+[0$\bar{1}$1] (and ($\bar{1}\bar{1}$1)[101]+[011]) CP systems are active. In fact, it seems that the CD system tends to put [114] parallel to ND to obtain the (114)[$\bar{2}\bar{2}$1] (and ($\bar{1}\bar{1}$4)[221]) orientation, knowing that this last orientation tends to the (112)[$\bar{1}\bar{1}$1] (and ($\bar{1}\bar{1}$2)[111]) one during plane strain compression as it has been seen above. Then, one can assume that the CP system counterbalances the CD one, and consequently, the (112)[$\bar{1}\bar{1}$1] and ($\bar{1}\bar{1}$2)[111] orientations remain stable during the deformation. At higher strains, the appearence of the (110)[001] can be linked with a rotation of whole MSBs around TD near a position parallel to the compression plane, corresponding to the development of the (111)[$\bar{1}\bar{1}$2] orientation. This component ([13, 18]) splits into the (112)[$\bar{1}\bar{1}$1] (which explains the stability of this orientation) and the (110)[001] orientations. When comparing the lattice rotations of figures 6a and 6b, we note that, for MSBs, the lattice inside the band rotates relatively more slowly than the surrounding crystal matrix lattice. The localized shear by combination of two coplanar slip systems is therefore favoured along the nearest critically stressed slip plane (111) at 35° to ED.

Jasienski et al. [3] showed that the Goss initial orientation is stable until about $\bar{\varepsilon}$=1.0 in plane strain compression, but spreads by rotation around the ND towards the (110)[1$\bar{1}\bar{2}$] orientation. (see also [1]). From Wrobel et al. [14], it is commonly accepted that (110)[001] f.c.c. single crystals are metastable during deformation by rolling. Moreover, it has been proved using the Sachs model, that under the conditions of plane stress state, this orientation is stable in relation to the rotation around RD and TD. However, it is unstable with respect to each one; even very slight fluctuations around ND cause rotation toward two symmetric stable end orientations (110) [1$\bar{1}\bar{2}$]. Morii et al. [7] observed the same phenomenon on (011)[$\bar{1}$00] Al-Mg crystals which were stable up to about 70 pct of reduction ($\bar{\varepsilon}$=1.39), and then tended to rotate around the sheet plane normal towards the (011)[$\bar{2}\bar{1}$1] orientation at higher reductions.

3.2. The (111)[$\bar{1}\bar{2}\bar{3}$] initial orientation

The evolution of the (111)[$\bar{1}\bar{2}$3] orientation during the compression is schematically plotted on figure 8. The first transformation of the (111)[$\bar{1}\bar{2}$3] orientation can be explained by a double rotation, which certainly occurs simultaneously during the deformation. However, for the sake of simplicity, they can be separated in the first step in a rotation of about 10° around ND which leads to the (111)[$\bar{1}\bar{1}$2] orientation, then, there appears a rotation of ± 15° around TD which leads to the (112)[$\bar{1}\bar{1}$1] and (552)[$\bar{1}\bar{1}$5] orientations, respectively. When the deformation increases, the evolution of the two last orientations can be still described by a rotation around TD. For the first one, the spreading reaches (114)[$\bar{2}\bar{2}$1] with a rotation of about 15°. Equal rotation of opposite sign is needed to transform the (552)[$\bar{1}\bar{1}$5] texture component to the (110)[001] orientation. Then, the Goss orientation spreads towards the (110)[1$\bar{1}\bar{2}$] one by a rotation of 35° around ND. Wonsiewicz and Chin [13] have already shown that the (111)[$\bar{1}\bar{1}$2] orientation can rotate either towards (112)[$\bar{1}\bar{1}$1] or towards (110)[001]. The sense of rotation is determined by the local stresses and the single crystal sample is observed to divide into four symmetrical parts, two of them having the final orientations.

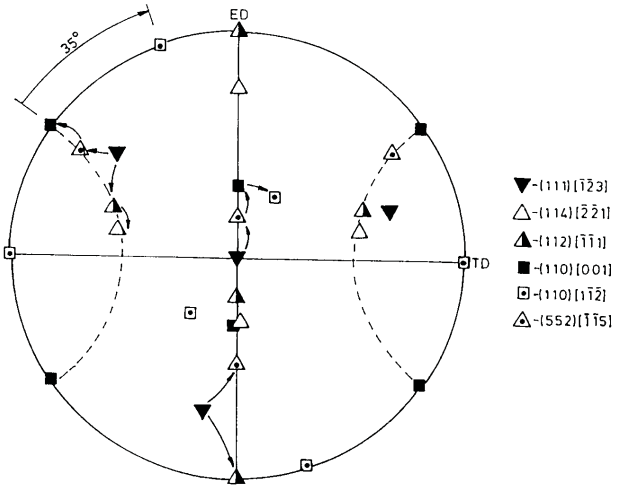

Fig. 8. Evolution of the (111)[$\bar{1}\bar{2}$3] initial orientation during deformation

This evolution of the (111)[$\bar{1}\bar{2}$3] orientation during deformation can be explained in terms of slip systems. Calculation of active slips using the Schmid law shows that the two (1$\bar{1}$1)[110] and (11$\bar{1}$)[101] slip systems are active at low strains. A rotation of about 10° around ND associated with these two systems leads to the (112)[$\bar{1}\bar{1}$1] and (552)[$\bar{1}\bar{1}$5] orientations.

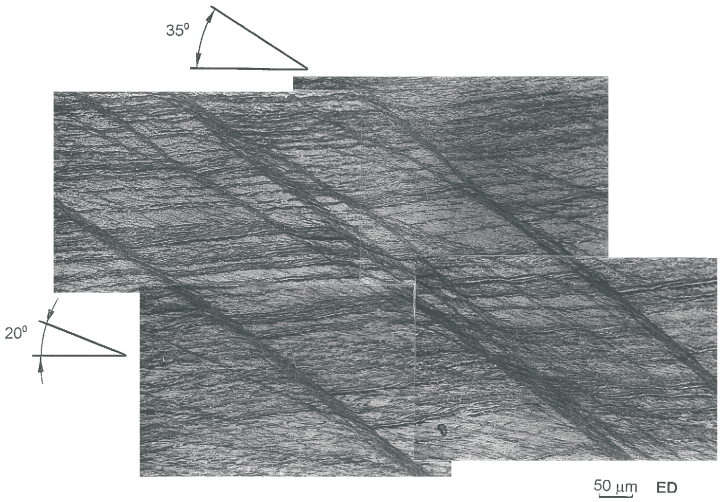

Fig. 9. (111)[$\bar{1}\bar{2}3$] initial orientation. Micrograph of the CSBs and the MSBs ($\overline{\varepsilon}$=1.35)

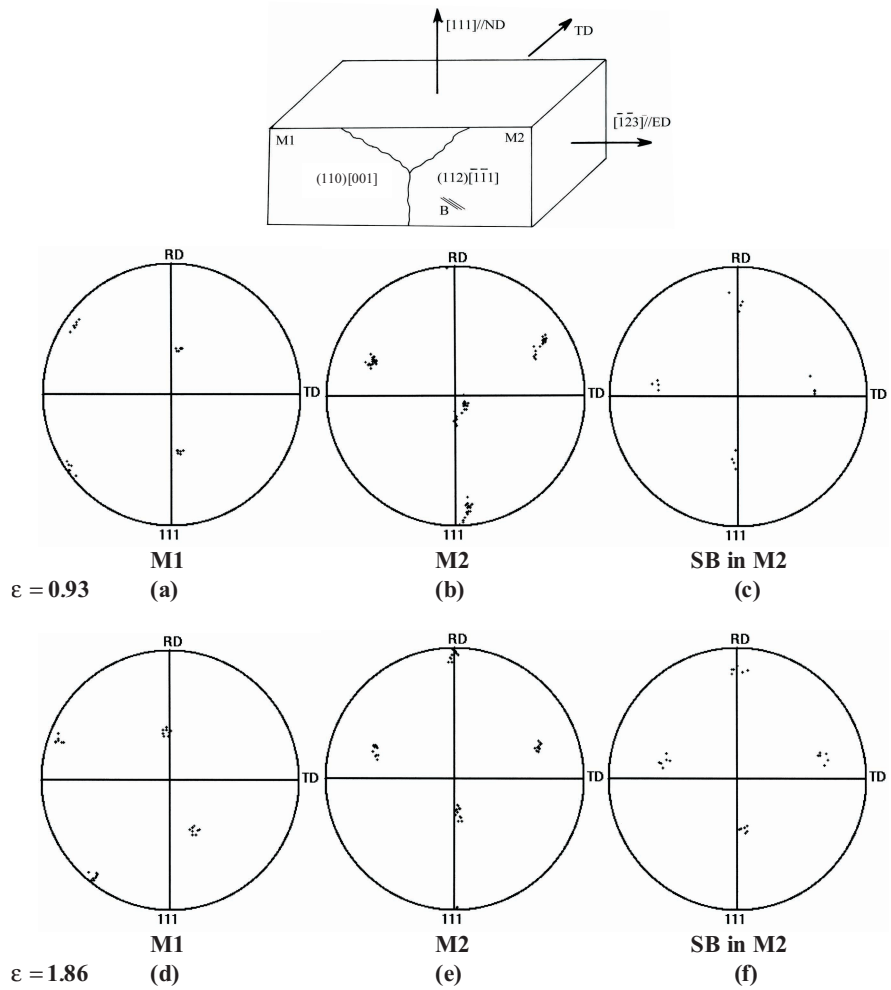

Fig. 10. (111)[$\bar{1}\bar{2}3$] initial orientation. {111} pole figures measured for a plane strain :
$\overline{\varepsilon}$=0.93 by EBSD (a) within the part of matrix M1, (b) within the part of matrix M2, (c) within the MSBs
$\overline{\varepsilon}$=1.86 by EBSD (d) within the part of matrix M1, (e) within the part of matrix M2, f) within the MSBs

The deformation of the crystal part of (112)[$\bar{1}\bar{1}$1] orientation (marked M2 in Fig.10) is performed on two pairs of slip systems: a ($\bar{1}$11)+(1$\bar{1}$1)[110] CD slip system and a (111)[$\bar{1}$01]+[0$\bar{1}$1] CP slip system. As already described during the study of the (001)[110] orientation, for the (112)[$\bar{1}\bar{1}$1] orientation, using the Schmid law, four slip systems lead to the stability of this orientation, thus, to obtain the (114)[$\bar{2}\bar{2}$1], the CD must be more active than the CP. Then, when the (114)[$\bar{2}\bar{2}$1] orientation is reached, only the CP slip system remains active leading to the appearance of the (112)[$\bar{1}\bar{1}$1] orientation.

The part of single crystal of the (552)[$\bar{1}\bar{1}$5] orientation (marked M1 in Fig.10) is deformed by a slip in the (11$\bar{1}$)[101]+[011] CP system which enables the appearance of the (110)[001] Goss orientation. For this last orientation, two pairs of (111)[10$\bar{1}$]+[01$\bar{1}$] and (11$\bar{1}$)[101]+[011] CP systems are symmetrically activated, leading to the stability of the Goss orientation.

Let us finally remark that, after the appearance of well developed MSBs ($\overline{\varepsilon}$=0.9), the (114)[$\bar{2}\bar{2}$1] and (110)[001] components are present in different fragments of deformed sample (Fig.10, part M2 and M1). For higher strains, the spreading of the (110)[001] orientation (Fig.10d, M1) by the rotation about the ND towards the (110)[1$\bar{1}\bar{2}$] orientation, which is stable, is due to an unbalanced slip in one of the CP systems. This symmetry loss of the active CP systems is perhaps connected with the appearance of friction stresses during the plane compression.

The EBSD allows one to distinguish the crystal matrix and the MSBs orientations. Figures 10a and 10b show the respective orientations measured in the MSBs and in two parts of single crystal matrix (M1 and M2), where the (112)[$\bar{1}\bar{1}$1] orientation remains stable (low spreading). The orientations measured in MSBs (in the part M2) are more scattered (Fig. 10c). There appears in the M2 part the (112)[$\bar{1}\bar{1}$1] orientation with a spreading towards (114)[$\bar{2}\bar{2}$1] and in M1 part the (110)[001] which splits towards the (110)[1$\bar{1}\bar{2}$] orientation. Since the (112)[$\bar{1}\bar{1}$1] texture component remains stable it seems that the Goss component derives from the (552)[$\bar{1}\bar{1}$5] orientation (Fig. 10a).

For the crystal deformed up to $\overline{\varepsilon}$=0.9, the local texture inside the MSBs measured by X-ray diffraction (as sketched in fig. 2) is shown in figure 11a. The results confirm, in particular, the appearance of the Goss orientation as a minor component of local texture and the pronounced splitting of the main C-component towards (114)[$\bar{2}\bar{2}$1] orientation.

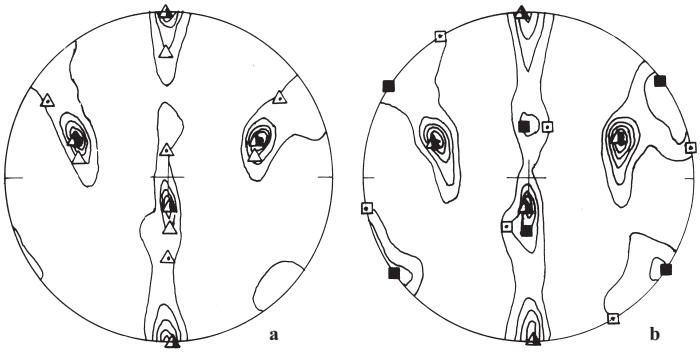

△ (114)[$\bar{2}\bar{2}$1]; ▲ (112)[$\bar{1}\bar{1}$1]; ■ (110)[001]; ⊡ (110)[1$\bar{1}$3]; ◬ (552)[$\bar{1}\bar{1}$5]

Fig. 11. {111}pole figures measured inside the MSBs by X-ray diffraction for plane strain (a) $\overline{\varepsilon}$ = 0,93, (b) $\overline{\varepsilon}$ = 1,86

At $\overline{\varepsilon}$ =1.86, the orientation spreading, determined by X-ray diffraction, in the MSBs is larger than that at *overline*ε =0.93 because there appear almost all the mentioned orientations (Fig.11b).

The EBSD allows one to distinguish in the matrix part M2 (Fig.10e) the presence of a sharp (112)[$\bar{1}\bar{1}$1] texture component with a spreading towards (114)[$\bar{1}\bar{1}$1] within the MSBs (Fig.10f). This spreading seems to be very important, but it is necessary to indicate that for large strains, it becomes difficult to measure with good precision, the individual orientations with the EBSD, since the size of dislocation cells tend to be smaller than the spatial resolution of the technique. However, it is interesting to remark that the presence of (552)[$\bar{1}\bar{1}$5] and (110)[001] orientations cannot be observed. On the other hand, an orientation between the (110)[001] and (110)[1$\bar{1}\bar{2}$] orientations is visible on the {111} pole figure measured in the matrix part M1 (fig. 10d).

A TEM analysis [3,4] has shown that the MSBs composed of microband clusters are closely aligned with the {111} common planes of the (114)[$\bar{2}\bar{2}$1] and (110)[001] orientation. The MSB plane is inclined by about 35° (fig. 12) with respect to the compression plane, which agrees well with the positions of the octahedric

planes (111) defined by these two components of local texture inside the band, i.e. these crystallographic planes also are at 35° to ED (fig. 13).

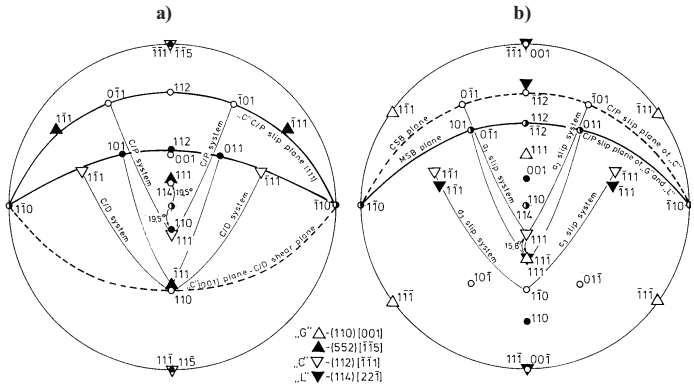

Fig. 12. (a) Superimposed stereographic projections of (112)[$\bar{1}\bar{1}1$] and (552)[$\bar{1}\bar{1}5$] orientations
(b) Superimposed stereographic projections of C-(112)[$\bar{1}\bar{1}1$], G-(110)[001] and L-(114)[2 2 $\bar{1}$] orientations

The misorientation of the octahedric planes {111} inside of individual MSBs appearing in the compressed sample of copper (112)[$\bar{1}\bar{1}1$] single crystals was measured by EBSD, on the plane (ND, RD) step by step along a line of 11000 μm long and parallel to RD. The figure 14 shows that inside of the shear band (SB) the maximum of disorientation is of about 15 deg. Consequently, it corresponds to the inclination of {111} planes inside MSBs by about 35° with respect to the compression/or rolling/ plane, because the inclination on of {111} in the matrix (M) of (112)[$\bar{1}\bar{1}1$] stable orientation is about 20°. The local spreading towards (114)[$\bar{2}\bar{2}1$] is distinctly observed from {111} pole figure measured inside the shear band (SB).

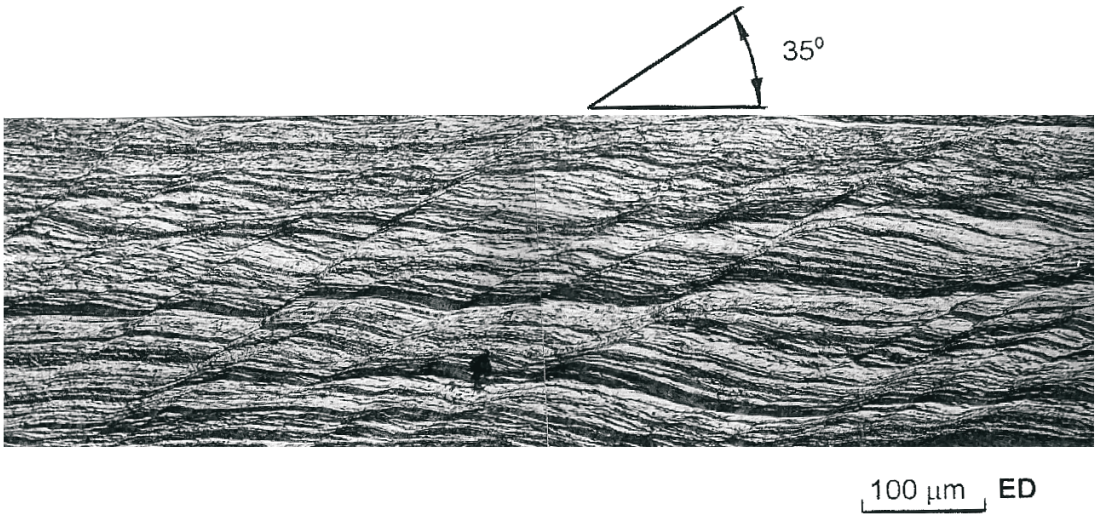

Fig. 13. (111)[$\bar{1}\bar{2}3$] initial orientation. Micrograph of the MSBs ($\bar{\varepsilon}$=2.0)

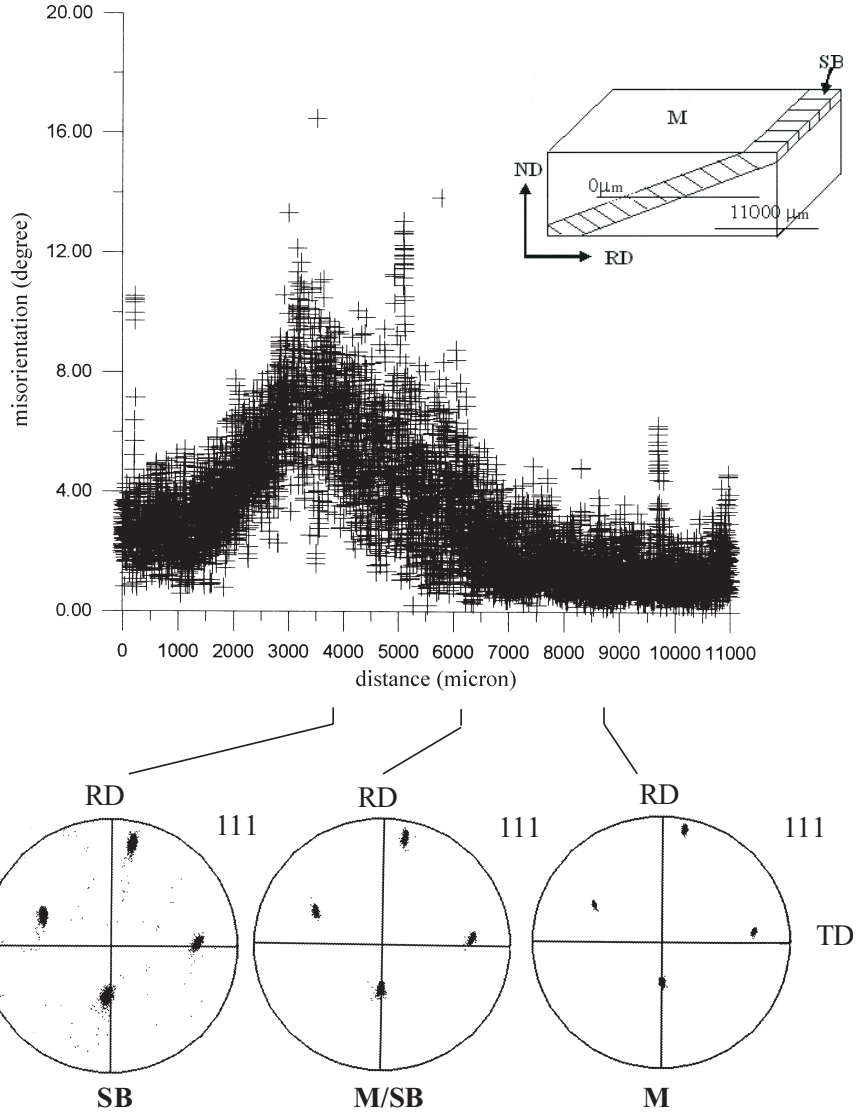

Fig. 14. Local misorientation inside the single shear band measured by EBSD in plane strain compressed (112)[$\bar{1}\bar{1}$1] copper single crystal

These results, obtained from individual measurements by EBSD, seem to prove the crystallographic nature of MSBs, which develop in deformed single crystals of C orientation.

TABLE
Plane strain compression value for the two studied single crystals

(001)[110]	(111)[$\bar{1}\bar{2}$3]
$\overline{\varepsilon}$	$\overline{\varepsilon}$
0.45	0.93
1.82	1.86

4. Conclusion

This study allows to elucidate some important points concerning the experimental methods and the evolution of the initial orientation of copper single crystals during plane strain compression :

(i) The EBSD technique is very useful for distinguishing the orientations of the crystal matrix from those of the slip or shear bands. In some cases, they can be determined or verified by X-diffraction, masking the matrix, if there exists only one set of bands. Indeed, this last method remains a global one and so it does not allow one to separate, for example, the two sets of CSBs which appear in the (001)[110] orientation.

(ii) From the metallurgical point of view, this method, coupled with the active slip systems analysis, has permitted to describe with a rather good precision the orientations and their location in the crystal matrix and in the slip or shear bands.

It has been shown, for the (001)[110] orientation, that the (112)[$\bar{1}\bar{1}$1] and ($\bar{1}\bar{1}$2)[111] orientations appear together with (114)[$\bar{2}\bar{2}$1] and ($\bar{1}\bar{1}$4)[221], respectively,

knowing that these orientations are located in two respective symmetric sets of MSBs.

For the (111)[$\bar{1}\bar{2}$3] orientation, the most important result refers to the development of the Goss orientation in the MSBs, as it has been verified using the EBSD technique.

REFERENCES

[1] S. V. Harren, H. E. Dève, R. J. Asaro, Acta Metall. **36**, 2435 (1998).

[2] M. Dao, R. J. Asaro, Scripta Metall. Mater. **30**, 791 (1994).

[3] Z. Jasienski, A. Piatkowski, Archives of Metall. **38**, 279 (1993).

[4] Z. Jasienski, A. Piatkowski, Proc. of the 9th International Conference on Strength of Metals and Alloys, Haifa, Eds D.G. Brandon et al., Freund Publ. **2**, 1025 (1991).

[5] J. H. Driver, D. Juul Jensen, N. Hansen, Acta Metall. Mater. **42**, 3105 (1994).

[6] Z. Jasienski, T. Baudin, Piatkowski, R. Penelle, Scripta Mater. **35**, 397 (1996).

[7] K. Morii, H. Mecking, Y. Nakayama, Acta Metall. **33**, 379 (1985).

[8] P. Wagner, N. Akdut, K. Lücke, G. Gottstein, Proc. of the 10th International Conference on Textures and Microstructures, Clausthal, Germany, 1993, Ed. H.J. Bunge, Materials Science Forum, 157-162, Part 1 865 (1994).

[9] P. Wagner, O. Engler, K. Lücke, Acta Metall. Mater. **43**, 3799 (1995).

[10] D. J. Dingley, Proc. of the 8th International Conference on Textures and Microstructures, Santa-Fé, USA, 1987, Ed. J.S. Kallend and G. Gottstein, TMS, Warrendale, PA 189 (1988).

[11] A. Akef, J. H. Driver, Mater. Sci. Eng. **A132**, 245 (1991).

[12] R. Becker, J. F. Butler, H. Hu, L. S. Lalli, Metall. Trans. **22A**, 45 (1991).

[13] B. C. Wonsiewicz, G. Y. Chin, Met. Trans. **1**, 2715 (1970).

[14] M. Wrobel, S. Dymek, M. Blicharski, S. Gorczyca, Textures and Microstructures **10**, 9 (1988).

[15] R. E. Bauer, H. Mecking, K. Lücke, Materials Science and Engineering **27**, 163 (1977).

[16] J. F. Butler, H. Hu, Materials Science and Engineering, **A114**, L29 (1989).

[17] G. D. Köhlhoff, J. Hirsch, U.v. Schlippenbach, K. Lücke, Proc. of the 6th International Conference on Textures and Microstructures, Tokyo, Japan, 1981, Ed. S. Nagashima, The Iron and Steel Institute 489 (1981).

[18] A. Akef, R. Fortunier, J. H. Driver, T. Watanabe, Proc. of the 9th International Conference on Textures and Microstructures, Avignon, France, 1990, Ed. H.J. Bunge, Textures and Microstructures **14-18**, 617 (1991).

Received: 20 December 2008.